Downloaded from jnm.snmjournals.org by on March 15, 2017. For personal use only.

Comparative Biodistribution and Radiation Dosimetry of ^{68}Ga-DOTATOC and ^{68}Ga-DOTATATE in Patients with Neuroendocrine Tumors

Mattias Sandström[1,2], Irina Velikyan[1,3], Ulrike Garske-Román[1,3], Jens Sörensen[1,3], Barbro Eriksson[4], Dan Granberg[4], Hans Lundqvist[5], Anders Sundin[6], and Mark Lubberink[1,2]

[1]Nuclear Medicine and PET, Uppsala University, Uppsala, Sweden; [2]Medical Physics, Uppsala University Hospital, Uppsala, Sweden; [3]Molecular Imaging, Uppsala University Hospital, Uppsala, Sweden; [4]Endocrine Oncology, Uppsala University, Uppsala, Sweden; [5]Biomedical Radiation Sciences, Uppsala University, Uppsala, Sweden; and [6]Radiology, Karolinska University Hospital, Stockholm, Sweden

^{68}Ga-DOTATOC and ^{68}Ga-DOTATATE are 2 radiolabeled somatostatin analogs for in vivo diagnosis of neuroendocrine tumors with PET. The aim of the present work was to measure their comparative biodistribution and radiation dosimetry. **Methods:** Ten patients diagnosed with neuroendocrine tumors were included. Each patient underwent a 45-min dynamic and 3 whole-body PET/CT scans at 1, 2, and 3 h after injection of each tracer on consecutive days. Absorbed doses were calculated using OLINDA/EXM 1.1. **Results:** Data from 9 patients could be included in the analysis. Of the major organs, the highest uptake at 1, 2, and 3 h after injection was observed in the spleen, followed by kidneys and liver. For both tracers, the highest absorbed organ doses were seen in the spleen and urinary bladder wall, followed by kidney, adrenals, and liver. The absorbed doses to the liver and gallbladder wall were slightly but significantly higher for ^{68}Ga-DOTATATE. The total effective dose was 0.021 ± 0.003 mSv/MBq for both tracers. **Conclusion:** The effective dose for a typical 100-MBq administration of ^{68}Ga-DOTATATE and ^{68}Ga-DOTATOC is 2.1 mSv for both tracers. Therefore, from a radiation dosimetry point of view, there is no preference for either tracer for PET/CT evaluation of somatostatin receptor–expressing tumors.

Key Words: biodistribution; dosimetry; ^{68}Ga-DOTATATE; ^{68}Ga-DOTATOC; neuroendocrine tumors

J Nucl Med 2013; 54:1755–1759
DOI: 10.2967/jnumed.113.120600

Neuroendocrine tumors can be diagnosed in vivo using PET with the radiolabeled somatostatin analogs ^{68}Ga-DOTATOC and ^{68}Ga-DOTATATE (*1,2*). Although the dosimetry of both tracers has been described separately (*3,4*) and has shown comparable effective doses, a comparative study using an identical, standardized methodology in a single group of patients has not been published and is of interest for tracer selection from a radiation dosimetry point of view. An earlier study did compare the biodistribution and radiation dosimetry of ^{111}In-labeled DOTATOC and DOTATATE (*5*) as estimated using whole-body scintigraphy. In that study, the main focus was to compare the 2 peptides with reference to their use in targeted peptide radiotherapy, mainly using ^{111}In as an analog for the therapeutic peptides ^{177}Lu-DOTATATE and ^{90}Y-DOTATOC. Similarly, DOTATOC labeled with the positron-emitting isotope ^{86}Y has been suggested as an analog of ^{90}Y-DOTATOC (*6*), but the complex decay scheme of ^{86}Y (*7*) makes it unfavorable as a diagnostic tracer. In contrast, the ^{68}Ga-labeled peptides will likely be used mainly for diagnosis and assessment of eligibility for somatostatin analog therapy. The diagnostic yield of the 2 tracers has been compared in 40 patients who underwent PET with both (*2*). In that study, tumor uptake of ^{68}Ga-DOTATOC was higher than that of ^{68}Ga-DOTATATE. Tumor detection was similar for the 2 tracers in a region-based analysis, but overall, significantly more lesions were found by ^{68}Ga-DOTATOC PET/CT. The aim of the present work was to use dynamic and serial whole-body PET/CT to measure the biodistribution and estimate the radiation dosimetry of ^{68}Ga-DOTATOC and ^{68}Ga-DOTATATE in a single group of patients.

MATERIALS AND METHODS

Patients

Ten patients (mean age, 62 y; range, 44–75 y; 6 men and 4 women) diagnosed with disseminated neuroendocrine tumors as confirmed by histopathology were included. Three of the patients had pancreatic neuroendocrine tumors, 5 had small-intestinal neuroendocrine tumors, and 2 had lung carcinoids. All patients signed a written informed consent form before inclusion, and the study was approved by the Regional Medical Ethics Board.

Tracer Production and Quality Control

Sodium acetate buffer (pH 4.6), sodium hydroxide (10 M), and doubly distilled hydrochloric acid (Riedel de Haën) were obtained from Sigma-Aldrich Sweden. Trifluoroacetic acid was obtained from Merck. The purchased chemicals were used without further purification. Commercially available DOTATOC and DOTATATE (Eurogentec S.A.) were dissolved in sterile water to give a 1 mM solution. ^{68}Ga (half-life, 68 min; β^+ decay, 89%; electron capture, 11%) was eluted with 0.6 M HCl from a ^{68}Ge/^{68}Ga-generator (1,850 MBq; IDB Holland BV), where ^{68}Ge (half-life, 270.8 d) was attached to a column of

Received Jan. 28, 2013; revision accepted May 2, 2013.
For correspondence or reprints contact: Mark Lubberink, PET Centre, Uppsala University Hospital, 751 85 Uppsala, Sweden.
E-mail: mark.lubberink@akademiska.se
Published online Aug. 8, 2013.
COPYRIGHT © 2013 by the Society of Nuclear Medicine and Molecular Imaging, Inc.

Downloaded from jnm.snmjournals.org by on March 15, 2017. For personal use only.

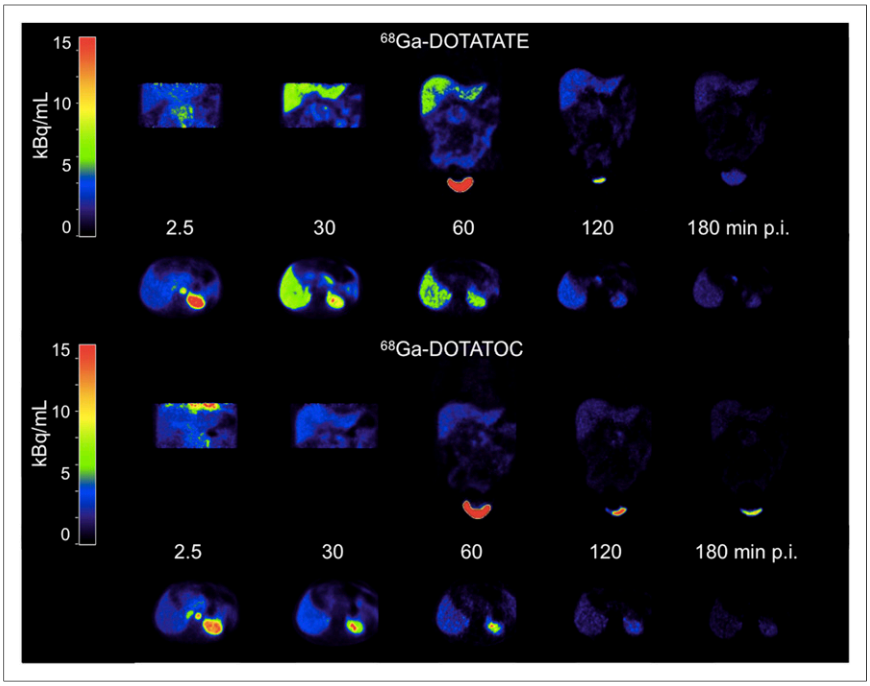

FIGURE 1. Representative images (not decay-corrected) at 0–5, 30, 60, 120, and 180 min after injection of 103 MBq of ^{68}Ga-DOTATATE and 100 MBq of ^{68}Ga-DOTATOC in same patient (patient with highest ^{68}Ga-DOTATATE liver residence time in Fig. 4) on 2 consecutive days. For both tracers, upper row is coronal slices and lower row is transversal slices.

an inorganic matrix based on tin dioxide. Production and quality control of the tracers were compliant with good manufacturing practices and were accomplished within 1 h. The fractionation method was used for the labeling (*8*). The first 1.0-mL fraction was sent to the waste, and the next 1.0 mL, containing over 65% of the total radioactivity, was collected and buffered with 200 μL of acetate buffer and 60 μL of sodium hydroxide to provide a pH of 4.6 ± 0.4. Radioactivity was measured, and 200–300 MBq were taken for the labeling synthesis. Thirty nanomoles of either DOTATOC or DOTATATE were added, and the reaction mixture was heated at 90°C–95°C for 10 min. The crude ^{68}Ga-DOTATOC and ^{68}Ga-DOTATATE were purified using a C8 (Sep-Pak Light; Waters) reversed solid-phase extraction cartridge. The product was eluted with 0.5 mL of 90% ethanol and formulated with sterile phosphate buffer (pH 7.4), and the resulting solution was passed through a 0.22-μm filter into a sterile injection vial. A sample was taken for determination of identity, radiochemical purity, chemical purity, and pH; for estimation of the peptide content, and for control of sterility and endotoxins.

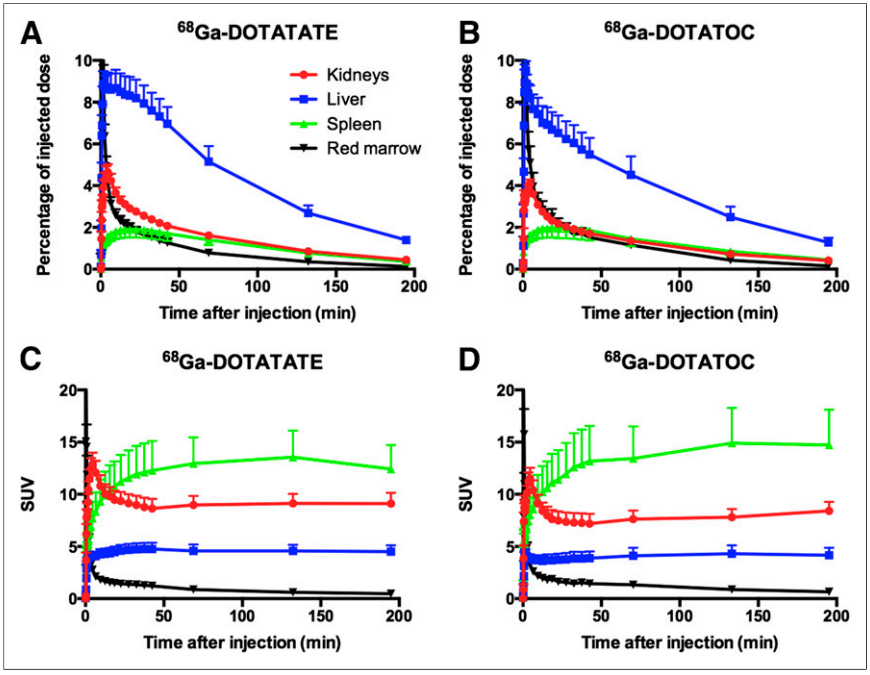

FIGURE 2. Percentage of injected activity (A and B) and SUV (C and D) as function of time after injection in kidneys, liver, spleen, and red marrow for ^{68}Ga-DOTATATE (A and C) and ^{68}Ga-DOTATOC (B and D). Error bars indicate SEs. SUV data were corrected for radioactive decay; percentage of injected dose data were not. Red marrow SUV is identical to whole-blood SUV.

PET Protocol

PET data were acquired using a Discovery ST (GE Healthcare) PET/CT scanner with an axial field of view of 15.7 cm. After a low-dose CT scan for patient positioning and attenuation correction, a 45-min dynamic PET scan (6 × 10, 4 × 60, 5 × 180, 5 × 300 s) over the abdominal region, including the liver, spleen, adrenals, and kidneys, was started simultaneously with the injection of either 91.4 ± 18.7 MBq (range, 72–120 MBq) of ^{68}Ga-DOTATATE or 86.9 ± 16.4 MBq (range, 62–112 MBq) of ^{68}Ga-DOTATOC. Three whole-body scans followed (proximal femur to base of skull), starting at 1, 2, and 3 h after injection, with scan durations of 3, 4, and 5 min per bed position, respectively, each preceded by a low-dose CT examination. Images were reconstructed using normalization and attenuation-weighted ordered-subsets expectation maximization (2 iterations, 21 subsets), including corrections for dead time, random coincidences as estimated by singles counting rates, model-based scatter correction (*9*), attenuation based on a bilinear conversion of Hounsfield units to 511-keV attenuation coefficients, and decay. A 5.4-mm gaussian postprocessing filter was applied. Venous blood samples were drawn after each whole-body scan for measurement of whole-blood radioactivity concentrations. Patients were allowed to urinate between the dynamic scan and each consecutive whole-body examination. Urine was collected and weighed, and radioactivity concentration was measured. Accurate cross-calibration between the PET/CT scanner, the dose calibrator, and the well counters that were used to measure blood and urine activity was verified monthly and was

Downloaded from jnm.snmjournals.org by on March 15, 2017. For personal use only.

TABLE 1
Residence Times (h) (n = 9)

Site	^{68}Ga-DOTATATE	^{68}Ga-DOTATOC
Kidney	0.056 ± 0.010	0.048 ± 0.011
Liver*	0.161 ± 0.056	0.128 ± 0.041
Spleen	0.038 ± 0.020	0.038 ± 0.023
Adrenal gland	0.003 ± 0.002	0.003 ± 0.001
Lungs	0.005 ± 0.001	0.006 ± 0.002
Urinary bladder contents	0.070 ± 0.045	0.086 ± 0.052
Bone marrow	0.032 ± 0.013	0.038 ± 0.016
Heart contents	0.012 ± 0.005	0.014 ± 0.005
SI contents	0.021 ± 0.008	0.018 ± 0.008
ULI contents	0.008 ± 0.003	0.007 ± 0.003
LLI contents	0.001 ± 0.000	0.001 ± 0.000
Remainder of body	1.152 ± 0.088	1.149 ± 0.079

*Significant difference between tracers (Wilcoxon signed-rank test; $P < 0.05$).

LLI = lower large intestine; SI = small intestine; ULI = upper large intestine.

always within 3%. The scan was repeated on the next day with the other tracer. The patients were randomized regarding the order of tracer used on the 2 consecutive examination days.

Volumes of Interest (VOIs)

VOIs were drawn at the same locations on the whole-body images and on the last time frame of the dynamic image series over clearly tumor-free subsets of all clearly identifiable source organs: liver, kidneys, spleen, lungs, small intestine, and adrenal glands. VOIs drawn on the last frame of the dynamic scans were transferred to all earlier time frames. Activity concentration and standardized uptake value (SUV) normalized to body mass and injected amount of radioactivity were determined using the mean activity concentration in VOIs. For adrenal glands, SUV was based on maximum pixel values because of their small volume and corresponding limited recovery.

For measurement of blood radioactivity concentrations during the dynamic scan, 1-cm-diameter circular regions of interest were drawn on 10 consecutive image planes over the descending aorta in the time frame where the first pass of the activity was best visualized and were combined to a single VOI. This VOI was then transferred to all other time frames in the dynamic scan and combined with blood samples collected at later time points to obtain a whole-blood time–activity curve.

Absorbed Dose Calculations

Red marrow radioactivity concentration was assumed to be equal to blood radioactivity concentration (*10*). Total organ activity was calculated by multiplying the radioactivity concentrations by the organ weights of the adult reference male or female phantom (*11*). Time-integrated activity in each organ was calculated by trapezoidal integration of the first 45 min of the organ's time–activity curve, followed by a single-exponential fit to the remaining data points (based on the 3 whole-body images) extrapolated to infinity, all based on non–decay-corrected data. For estimation of urinary bladder contents, all urine measurements were decay-corrected to the time of injection. Then, the bladder content at intermediate time points was estimated assuming linear filling of the bladder until each complete voiding. After the last scan, a 4-h voiding interval with filling rates equivalent to those before the last measured urine sample was assumed. This urinary bladder content time–activity curve was then uncorrected for decay, and time-integrated activity was calculated as the area under this time–activity curve. Residence times were obtained by dividing the time-integrated activity by the injected amount of activity. Small intestine, upper large intestine, and lower large intestine residence times were estimated using the ICRP 30 gastrointestinal tract model (*12*). Remainder-of-body activity was calculated as the injected activity minus the sum of the activity in all source organs and the activity excreted to urine up to each measurement point. Absorbed doses were calculated using OLINDA/EXM 1.1 (*13*).

Statistical Analysis

Differences between residence times and absorbed doses for both tracers were assessed using a Wilcoxon matched-pairs signed rank test. Differences between absorbed doses in male and female subjects were assessed using a Mann–Whitney test. A P value below 0.05 was considered significant. No multiple-comparisons correction was applied.

RESULTS

One patient (female) had to be excluded from analysis because of atypical biodistribution caused by a horseshoe kidney. Figure 1 shows typical whole-body images for both tracers. Figure 2 shows the biodistribution, in terms of SUV and percentage injected activity per organ, for ^{68}Ga-DOTATOC and ^{68}Ga-DOTATATE. Of the major organs, the highest SUV at 60–180 min after injection was observed in the spleen, followed by kidneys and liver. Clearance from the liver and kidney was slightly faster for ^{68}Ga-DOTATOC, resulting in a lower residence time in the liver ($P < 0.05$), whereas blood clearance was faster for ^{68}Ga-DOTATATE. Residence times, as shown in Table 1, were highest for the liver, followed by kidney, spleen, and urinary bladder contents.

During the first 4 h after injection, 15.6% (SD, 9.2) and 11.9% (SD, 4.1) of injected activity were excreted to urine for ^{68}Ga-DOTATOC and ^{68}Ga-DOTATATE, respectively. These percentages are in agreement with the slightly faster kidney clearance seen for ^{68}Ga-DOTATOC. However, there was no significant difference between excreted fractions.

Absorbed dose estimates are shown in Figure 3 and, for selected organs, in Table 2. The highest absorbed organ doses were seen in the spleen and urinary bladder wall, followed by the kidney, adrenals, and liver, for both tracers. Figure 4 compares residence times and absorbed doses in kidney and liver, as well as effective dose, for each individual patient. The total effective dose was 0.021 mSv/MBq for both tracers. When men

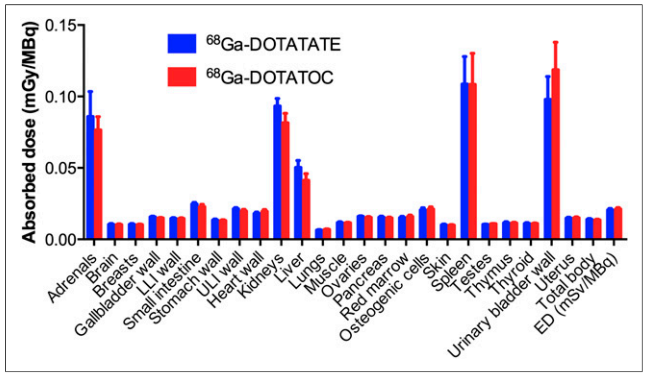

FIGURE 3. Absorbed doses in all organs included in OLINDA/EXM 1.1. Error bars indicate SEs. LLI = lower large intestine; ULI = upper large intestine; ED = effective dose.

Downloaded from jnm.snmjournals.org by on March 15, 2017. For personal use only.

TABLE 2
Absorbed Doses (mGy/MBq) in Selected Organs ($n = 9$)

Site	^{68}Ga-DOTATATE	^{68}Ga-DOTATOC
Kidney	0.093 ± 0.016	0.082 ± 0.020
Liver*	0.050 ± 0.015	0.041 ± 0.014
Gallbladder wall*	0.016 ± 0.002	0.015 ± 0.001
Spleen	0.109 ± 0.058	0.108 ± 0.065
Adrenal gland	0.086 ± 0.052	0.077 ± 0.028
Lungs	0.006 ± 0.001	0.007 ± 0.001
Urinary bladder wall	0.098 ± 0.048	0.119 ± 0.058
Red marrow	0.015 ± 0.003	0.016 ± 0.003
Total body*	0.014 ± 0.002	0.014 ± 0.002
Effective dose (mSv/MBq)	0.021 ± 0.003	0.021 ± 0.003

*Significant difference between tracers (Wilcoxon signed-rank test; $P < 0.05$).

and women were analyzed separately, effective doses of ^{68}Ga-DOTATATE and ^{68}Ga-DOTATOC were 0.020 and 0.020 mSv/MBq, respectively, for men and 0.022 and 0.023 mSv/MBq, respectively, for women ($P = 0.30$ and $P = 0.26$ for ^{68}Ga-DOTATATE and ^{68}Ga-DOTATOC, respectively). These values would result in an effective dose of 2.1 mSv for the typical 100-MBq amount administered in the present work. Absorbed doses to the liver, gallbladder wall, and total body were significantly higher for ^{68}Ga-DOTATATE (Wilcoxon matched-pairs signed rank test, $P < 0.05$, with higher absorbed doses for ^{68}Ga-DOTATATE in 7 of 9 and 8 of 9 patients, respectively), although absolute differences were small for the gallbladder wall (3%) and total body (1%).

DISCUSSION

To our knowledge, the present work is the first comparative study of the radiation dosimetry of ^{68}Ga-DOTATOC and ^{68}Ga-DOTATATE in a single group of patients. Radiation-absorbed doses were estimated using a protocol combining dynamic PET and serial whole-body PET scans in 9 patients. For both tracers, an effective dose of 2.1 mSv for a typical 100-MBq administration was found, with the only significant, although minor, difference in organ doses being seen for the liver and gallbladder wall. Residence times and absorbed doses in the kidney and liver were higher for ^{68}Ga-DOTATATE in 7 of 9 patients. The opposite was observed for effective dose, although differences in the effective dose of both tracers were minor even within individual patients (Fig. 4). The organ receiving the highest absorbed dose was the spleen for ^{68}Ga-DOTATATE and the urinary bladder wall for ^{68}Ga-DOTATOC. In both cases, the mean absorbed dose to these organs was about 20% of the maximum allowed dose of 50 mGy to a single organ in an adult research subject (*14*).

As can be seen in Figures 2 and 3, SUVs in the liver, kidney, and spleen are approximately constant starting at about 1 h after injection. Exponential fits to the last 3 measured data points resulted in effective half-lives slightly longer than the physical half-life of ^{68}Ga (~70 min and 75 min in liver and kidney for ^{68}Ga-DOTATATE and ^{68}Ga-DOTATOC, respectively). Since the scan protocol covered the major part of the radioactive decay of ^{68}Ga, the remaining decays after the last scan amount to at most a small percentage of the total number of disintegrations in each organ. Therefore, uncertainty in extrapolation after the 3-h whole-body scan only has minor effects on the total estimate of the time-integrated activity.

The patients included in the present work all had disseminated neuroendocrine tumor disease, mainly in the liver, mesenterically and retroperitoneally. Although we selected patients with limited tumor burden, that is, without bulky disease, uptake in tumors may have resulted in somewhat decreased availability of tracer for uptake into normal tissues. Tumor tissue is not explicitly accounted for when OLINDA/EXM 1.1 is used to assess radiation dosimetry, but activity in tumor tissue is included in the analysis as part of the remainder of the body.

Forrer et al. (*5*) compared the radiation dosimetry of ^{111}In-labeled DOTATOC and DOTATATE in a single patient group using planar whole-body scintigraphy and found results comparable to those in the present work, with higher kidney and liver doses for ^{111}In-DOTATATE and higher urinary excretion for ^{111}In-DOTATOC. Hartmann et al. (*3*) studied the radiation dosimetry of ^{68}Ga-DOTATOC in 14 patients and found a slightly higher effective dose of 0.023 mSv/MBq, with the spleen and kidney receiving much higher absorbed doses than in the present work (0.24 and 0.22 mGy/MBq in the study of Hartmann et al., compared with 0.11 and 0.08 mGy/MBq in our work), using a scanning protocol with sparser sampling requiring extrapolation over a larger fraction of the total decay of the tracer. The higher absorbed doses in the spleen and kidney correspond to proportionally higher SUVs in those organs in their work than in the present work. Walker et al. (*4*) evaluated the radiation dosimetry of ^{68}Ga-DOTATATE in merely 3 patients, using only whole-body scans at 30, 60, and 90 min after injection, and although the relative distribution of residence times and absorbed doses across organs was similar to the present study, they reported overall slightly higher organ doses and a higher effective dose (0.025 mSv/MBq) than in the present work. This difference may be caused by the extrapolation required for the first 30 min after injection and the shorter duration of their protocol compared with ours, necessitating extrapolation over a larger fraction of the total decay of the tracer as well. For comparison, Pettinato et al. found a somewhat lower effective dose of 0.017 mSv/MBq for ^{68}Ga-DOTANOC (*15*), a third somatostatin analog that has been suggested because of its highest combined affinity to different somatostatin receptor subtypes (*1*).

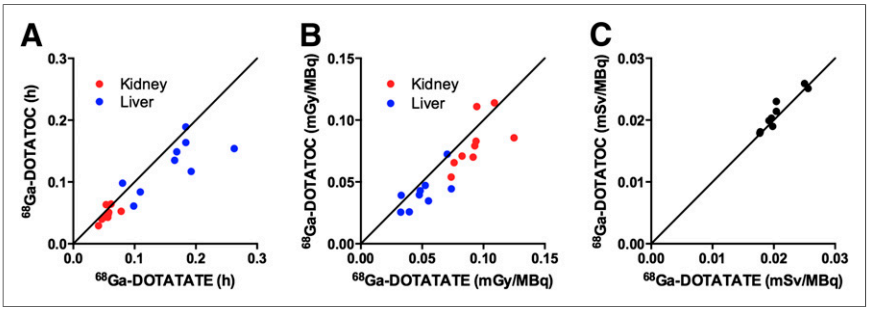

FIGURE 4. (A and B) Residence times (A) and absorbed doses (B) in kidney and liver. (C) Effective dose for ^{68}Ga-DOTATATE and ^{68}Ga-DOTATOC. Solid line in each panel is line of identity.

Downloaded from jnm.snmjournals.org by on March 15, 2017. For personal use only.

CONCLUSION

The effective dose for a typical 100-MBq administration of ^{68}Ga-DOTATATE and ^{68}Ga-DOTATOC is 2.1 mSv for both tracers, with only minor differences in doses to individual organs. Therefore, there is no preference for either tracer in the diagnoses and pretreatment evaluation of somatostatin receptor–expressing tumors in terms of radiation doses.

DISCLOSURE

The costs of publication of this article were defrayed in part by the payment of page charges. Therefore, and solely to indicate this fact, this article is hereby marked "advertisement" in accordance with 18 USC section 1734. Financial support was provided by Uppsala University Hospital and by the Swedish Cancer Society (grant CAN2011/580). No other potential conflict of interest relevant to this article was reported.

ACKNOWLEDGMENTS

We thank Mimmi Lidholm, Annie Bjurebäck, Maj Wiberg, Lars Lindsjö, and Marie Åhlman for their technical assistance in performing the scans.

REFERENCES

1. Breeman WA, de Blois E, Sze Chan H, Konijnenberg M, Kwekkeboom DJ, Krenning EP. ^{68}Ga-labeled DOTA-peptides and ^{68}Ga-labeled radiopharmaceuticals for positron emission tomography: current status of research, clinical applications, and future perspectives. *Semin Nucl Med.* 2011;41:314–321.
2. Poeppel TD, Binse I, Petersenn S, et al. ^{68}Ga-DOTATOC versus ^{68}Ga-DOTATATE PET/CT in functional imaging of neuroendocrine tumors. *J Nucl Med.* 2011;52:1864–1870.
3. Hartmann H, Zophel K, Freudenberg R, et al. Radiation exposure of patients during ^{68}Ga-DOTATOC PET/CT examinations [in German]. *Nuklearmedizin.* 2009;48:201–207.
4. Walker RC, Smith GT, Stabin M. First report of measured human dosimetry with ^{68}Ga-DOTATATE [abstract]. *J Nucl Med.* 2012;53(suppl):330P.
5. Forrer F, Uusijarvi H, Waldherr C, et al. A comparison of ^{111}In-DOTATOC and ^{111}In-DOTATATE: biodistribution and dosimetry in the same patients with metastatic neuroendocrine tumours. *Eur J Nucl Med Mol Imaging.* 2004;31:1257–1262.
6. Jamar F, Barone R, Mathieu I, et al. ^{86}Y-DOTA$_0$-D-Phe1-Tyr3-octreotide (SMT487): a phase 1 clinical study—pharmacokinetics, biodistribution and renal protective effect of different regimens of amino acid co-infusion. *Eur J Nucl Med Mol Imaging.* 2003;30:510–518.
7. Herzog H, Tellmann L, Scholten B, Coenen HH, Qaim SM. PET imaging problems with the non-standard positron emitters yttrium-86 and iodine-124. *Q J Nucl Med Mol Imaging.* 2008;52:159–165.
8. Velikyan I, Beyer GJ, Langstrom B. Microwave-supported preparation of ^{68}Ga-bioconjugates with high specific radioactivity. *Bioconjug Chem.* 2004;15:554–560.
9. Watson CC. New, faster, image-based scatter correction for 3D PET. *IEEE Trans Nucl Sci.* 2000;47:1587–1594.
10. Forrer F, Krenning EP, Kooij PP, et al. Bone marrow dosimetry in peptide receptor radionuclide therapy with [^{177}Lu-DOTA$_0$,Tyr$_3$]octreotate. *Eur J Nucl Med Mol Imaging.* 2009;36:1138–1146.
11. Stabin MG. MIRDOSE: personal computer software for internal dose assessment in nuclear medicine. *J Nucl Med.* 1996;37:538–546.
12. *ICRP Publication 30: Limits for Intakes of Radionuclides by Workers.* Ottawa, Canada: International Commission on Radiological Protection; 1980.
13. Stabin MG, Sparks RB, Crowe E. OLINDA/EXM: the second-generation personal computer software for internal dose assessment in nuclear medicine. *J Nucl Med.* 2005;46:1023–1027.
14. U.S. Food and Drug Administration Web site. Code of Federal Regulations Title 21, Section 361.1: Radioactive drugs for certain research uses. http://www.accessdata.fda.gov/scripts/cdrh/cfdocs/cfcfr/CFRSearch.cfm?FR=361.1. Revised April 1, 2013. Accessed July 25, 2013.
15. Pettinato C, Sarnelli A, Di Donna M, et al. ^{68}Ga-DOTANOC: biodistribution and dosimetry in patients affected by neuroendocrine tumors. *Eur J Nucl Med Mol Imaging.* 2008;35:72–79.

Downloaded from jnm.snmjournals.org by on March 15, 2017. For personal use only.

The Journal of NUCLEAR MEDICINE

Comparative Biodistribution and Radiation Dosimetry of ^{68}Ga-DOTATOC and ^{68}Ga-DOTATATE in Patients with Neuroendocrine Tumors

Mattias Sandström, Irina Velikyan, Ulrike Garske-Román, Jens Sörensen, Barbro Eriksson, Dan Granberg, Hans Lundqvist, Anders Sundin and Mark Lubberink

J Nucl Med. 2013;54:1755-1759.
Published online: August 8, 2013.
Doi: 10.2967/jnumed.113.120600

This article and updated information are available at:
http://jnm.snmjournals.org/content/54/10/1755

Information about reproducing figures, tables, or other portions of this article can be found online at:
http://jnm.snmjournals.org/site/misc/permission.xhtml

Information about subscriptions to JNM can be found at:
http://jnm.snmjournals.org/site/subscriptions/online.xhtml

The Journal of Nuclear Medicine is published monthly.
SNMMI | Society of Nuclear Medicine and Molecular Imaging
1850 Samuel Morse Drive, Reston, VA 20190.
(Print ISSN: 0161-5505, Online ISSN: 2159-662X)

© Copyright 2013 SNMMI; all rights reserved.

SNMMI SOCIETY OF NUCLEAR MEDICINE AND MOLECULAR IMAGING